



HAL
open science

Global linear stability analysis of kinetic Trapped Ion Modes (TIM) and their nonlinear saturation in tokamak plasma

Debraj Mandal, Maxime Lesur, Etienne Gravier, Juvert Njeck Sama,
Alejandro Guillevic, Yanick Sarazin, Xavier Garbet

► To cite this version:

Debraj Mandal, Maxime Lesur, Etienne Gravier, Juvert Njeck Sama, Alejandro Guillevic, et al.. Global linear stability analysis of kinetic Trapped Ion Modes (TIM) and their nonlinear saturation in tokamak plasma. 49th Conference on Plasma Physics, European Physical Society, Jul 2023, Bordeaux, France. hal-04597456

HAL Id: hal-04597456

<https://hal.univ-lorraine.fr/hal-04597456>

Submitted on 2 Jun 2024

HAL is a multi-disciplinary open access archive for the deposit and dissemination of scientific research documents, whether they are published or not. The documents may come from teaching and research institutions in France or abroad, or from public or private research centers.

L'archive ouverte pluridisciplinaire **HAL**, est destinée au dépôt et à la diffusion de documents scientifiques de niveau recherche, publiés ou non, émanant des établissements d'enseignement et de recherche français ou étrangers, des laboratoires publics ou privés.

Global linear stability analysis of kinetic Trapped Ion Modes (TIM) and their nonlinear saturation in tokamak plasma

D. Mandal¹, M. Lesur¹, E. Gravier¹, J. N. Sama¹, A. Guillevic¹, Y. Sarazin², X. Garbet^{2,3}

¹ *Université de Lorraine, CNRS, IJL, F-54000 Nancy, France*

² *CEA, IRFM, F-13108, Saint-Paul-lez-Durance, France*

³ *School of Physical and Mathematical Sc., NTU, 637371 Singapore*

Trapped ion modes (TIM) belong to the family of ion temperature gradient (ITG) modes which are one of the main instabilities that govern heat turbulent transport at the ion scale in tokamak plasmas. Trapped electron mode (TEM) turbulence drives electron particle and heat transport. In an unstable system, the most unstable mode grows by extracting free energy from the system which finally cascades into other higher and lower modes during nonlinear evolution. Therefore it is essential to properly estimate their linear growth rate to understand their influence on turbulent transport. For studying the TIM we have considered a reduced 4-dimensional gyrokinetic model with averaging over gyro-motion and the banana orbit, and adiabatic response of passing particles [3]. According to this model the gyro-bounce averaged Vlasov Equation can be written as,

$$\frac{\partial \bar{f}_s}{\partial t} - \left[J_{0,s} \phi, \bar{f}_s \right]_{\alpha, \psi} + \frac{\Omega_D(\psi, \kappa) E}{Z_s} \frac{\partial \bar{f}_s}{\partial \alpha} = 0. \quad (1)$$

\bar{f}_s is the banana centric distribution function for the species s . $J_{0,s}$ is the gyro-bounce average operator. $[\dots]_{\alpha, \psi}$ is the Poisson bracket in the phase space of toroidal precession angle α and poloidal magnetic flux ψ . In this model ψ is used as radius ($\psi \sim -r^2$). Ω_D is the precession frequency of the particle which is function of magnetic flux ψ , and the trapping parameter κ . κ can vary between 0 (for deeply trapped particles) to 1 (at separatrix for barely trapped particle). In this manuscript we consider only $\kappa = 0$. In equilibrium condition three constant of motions are Energy E , magnetic moment μ and toroidal kinetic momentum P_Φ . The potential ϕ is calculated from the quasi-neutrality equation [3]. In all the previous study, this gyro-bounce averaged model is simplified by considering $H_{eq} \approx E$ in both quasi-neutrality equation and equilibrium gyro-bounce averaged distribution function F_{eq} . This approximation is valid for $\psi = 0$ and precession frequency Ω_D doesn't depends on ψ . In this present study, the radial profile of the particle drift velocity is taken into account by considering the magnetic flux ψ dependency of the equilibrium Hamiltonian $H_{eq}(\psi)$ in both the quasi-neutrality equation and equilibrium gyro-bounce averaged distribution function F_{eq} .

Modification due to radial variation of precession motion

The magnetic flux ψ dependent expression for equilibrium Hamiltonian is,

$$\bar{H}_{eq}(\psi, \kappa) = E \left(1 + \int_0^\psi \Omega_D(\tilde{\psi}, \kappa) d\tilde{\psi} \right) = E\Lambda_D(\psi, \kappa), \quad (2)$$

where we define $\Lambda_D = \left(1 + \int_0^\psi \Omega_D(\tilde{\psi}, \kappa) d\tilde{\psi} \right)$. With this new equilibrium Hamiltonian the equilibrium banana centric distribution function becomes,

$$F_{eq,s}(\psi, E, \kappa) = \frac{n_{eq,s}(\psi)}{T_{eq,s}^{3/2}(\psi)} \exp\left(-\frac{E\Lambda_D(\psi, \kappa)}{T_{eq,s}(\psi)}\right). \quad (3)$$

With this new equilibrium Hamiltonian the elementary phase-space volume can be written as $d^3v = 4\pi\sqrt{2}m^{-3/2}\sqrt{E}\Lambda_D^{3/2}dE\frac{d\lambda}{4\Omega_D}$, where λ is the pitch angle. Using this new elementary volume element expression the modified quasineutrality condition can be written as,

$$\frac{2\Lambda_D(\psi, \kappa)^{3/2}}{\sqrt{\pi}n_{eq}(0)} \sum_s Z_s \int_0^1 \kappa \mathcal{K}(\kappa^2) d\kappa \int_0^\infty J_{0,s} f_s \sqrt{E} dE = \sum_s \frac{eZ_s^2}{T_{eq,s}(0)} \left[\frac{1-f_t}{f_t} (\phi - \varepsilon_{\phi,s} \langle \phi \rangle_\alpha) - \bar{\Delta}_s \phi \right], \quad (4)$$

where $\mathcal{K}(\kappa^2)$ is the complete elliptic function of first kind. $\bar{\Delta}$ is a non-isotropic Laplacian operator [3]. The expression for Vlasov Eq. (1), remain unchanged with this new Hamiltonian.

Global linear analysis: spectral method

A global linear analysis of this 4D-reduced model is performed to account for the radial boundary conditions. A spectral method based on [2], is proposed to solve the linear dispersion relation for calculating real part of frequency ω_r and growth-rate γ of different TIM modes n . We consider small amplitude perturbation of \bar{f} and $\bar{\phi}$, as $\tilde{f}_s = \sum_{n,\omega} f_{s,n,\omega}(\psi) \exp\{i(n\alpha - \omega t)\}$ and $\tilde{\phi} = \sum_{n,\omega} \phi_{n,\omega}(\psi)$. From the linearised Vlasov equation the solution $f_{n,\omega}$ can be written as function of potential $\phi_{n,\omega}$ in Fourier space (n is the mode no. along α). Using this $f_{n,\omega}$ in the quasi-neutrality condition, we can write a 2nd-order differential equation for ϕ_n as [1],

$$\frac{d^2 \phi_n}{d\psi^2} + Q_n(\psi) \phi_n = 0, \quad (5)$$

$$\text{with } Q_n(\psi) = \frac{\mathcal{N}_{n,i}^* - \frac{\sqrt{\pi}}{2T_i(0)} \left[C_{ad} + C_{pol}(\rho_i^{*2} + \tau\rho_e^{*2})n^2 \right]}{\frac{\sqrt{\pi}}{2T_i(0)} C_{pol}(\delta_{bi}^2 + \tau\delta_{be}^2)} \quad \text{and}$$

$$\mathcal{N}_n^* = \frac{\Lambda_D^{3/2}}{n_s(0)} \int_0^\infty \sqrt{E} J_{0,n} \left[\frac{n_s(\psi)}{T^{3/2}} \exp\left(-\frac{E\Lambda_D}{T}\right) \frac{\kappa_n + \kappa_T \left(\frac{E\Lambda_D}{T} - \frac{3}{2}\right) - \kappa_\Lambda \frac{E\Lambda_D}{T}}{Z^{-1}\Omega_D(\psi)(E - \chi)} J_{0,n} \right] dE,$$

is an differential operator acting on $\phi_{n,\omega}$ [1], where $\kappa_n = \frac{1}{n_s(\psi)} \frac{dn_s}{d\psi}$, $\kappa_T = \frac{1}{T_s(\psi)} \frac{dT_s}{d\psi}$ and $\kappa_\Lambda = \frac{1}{\Lambda_D(\psi)} \frac{d\Lambda_D}{d\psi} = \frac{\Omega_D(\psi)}{\Lambda_D(\psi)}$ are the logarithmic gradients of density, temperature and equilibrium Hamiltonian $H_{eq}(\psi)$, respectively. $C_{pol} = \frac{q_i \omega_0 L_\psi}{T_0}$, $C_{ad} = \frac{1-f_t}{f_t} (1 - \tau) C_{pol}$, $\tau = \frac{T_i}{T_e} \Big|_{\psi=0}$, $\chi = \frac{\omega}{nZ^{-1}\Omega_D(\psi)}$, and $\omega = \omega_r + i\gamma$. The quantity $(E - \chi_s)$ in denominator gives a resonance condition. For ions the resonance occurs only when $\omega > 0$, ie. the wave propagates along ion precession drift.

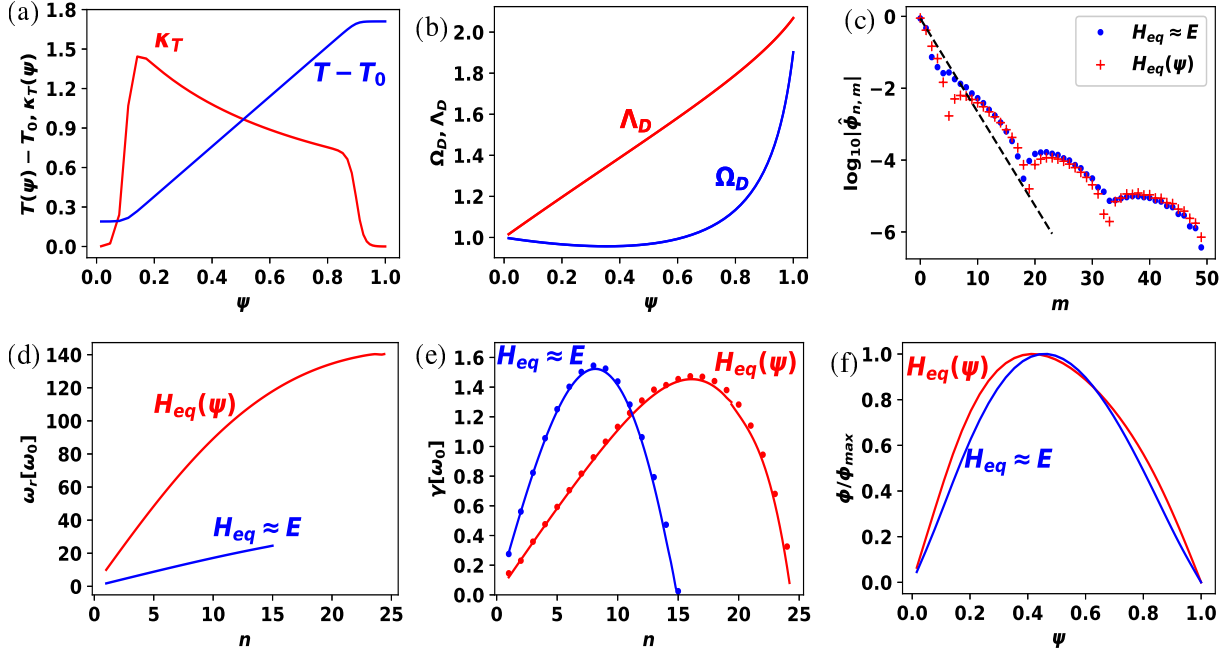


Figure 1: (a) Blue: Temperature profile ($T(\psi) - T_0$) where $T_0 = 1$. Red: $\kappa_T(\psi)$ profile. The gradient in $T(\psi)$ profile $G_T = 1.9$ (for $H_{eq}(\psi)$ case) and $G_T = 0.19$ (for $H_{eq} \approx E$ case). (b) Blue: $\Omega_D(\psi)$ profile, and red: $\Lambda_D(\psi)$ profile, which are used for the case $H_{eq}(\psi)$. For $H_{eq} \approx E$ case we choose $\Omega_D = 1$ and $\Lambda_D = 1$. (c) Spectral convergence of $\hat{\phi}_{n,m}$ for $H_{eq}(\psi)$ (red + markers) and $H_{eq} \approx E$ (blue dots). In both the cases they follow $|\hat{\phi}_{n,m}| \sim A_0 \exp(-\beta m)$ (black dashed line), with $\beta = 0.6$. (d) real part of frequency ($\omega_r - n$), for $H_{eq}(\psi)$ (red line) and $H_{eq} \approx E$ (blue line). For $H_{eq} \approx E$: $\omega_r \sim 2n$ and for $H_{eq}(\psi)$: $\omega_r \sim 10n$ (for $n < 10$). (e) growth-rate ($\gamma - n$), for $H_{eq}(\psi)$ (red line) and $H_{eq} \approx E$ (blue line). Dots: data from the TERESA simulations. (f) potential solution $\phi(\psi)$. Red line: $H_{eq}(\psi)$ case. Blue line: $H_{eq} \approx E$ case.

Spectral method

According to spectral method solution ϕ_n of Eq. 5 can be expressed as, $\phi_n(\psi) = \sum_{m=1}^M \hat{\phi}_{n,m} \mathcal{C}_m(\psi)$. The convergence of this method suggests, coefficients $\hat{\phi}_{n,m}$ should be go down exponentially towards zero, and $\hat{\phi}_{n,m=M} \approx 0$. We choose orthogonal polynomials, Chebyshev polynomials of first kind $T_{2(m-1)}$, for constructing \mathcal{C}_m as, $\mathcal{C}_m(\psi) = \psi(1 - \psi^2)T_{2(m-1)}(\psi)$. Using this choice Eq. 5 can be written as,

$$\sum_{m=1}^M \hat{\phi}_{n,m} \frac{d^2 \mathcal{C}_m(\psi)}{d\psi^2} = - \sum_{m=1}^M \hat{\phi}_{n,m} \mathcal{Q}_n(\psi) \mathcal{C}_m(\psi), \quad (6)$$

where m is the index of the spectral function \mathcal{C}_m , and n is wave number of TIM. We solve this Eq.(6), at the the collocation points, $\psi_l = \cos\left(\frac{(2l-1)\pi}{4M}\right)$ for $l \in \{1, \dots, M\}$, where first dropped higher order term of the expansion, namely the term \mathcal{C}_{M+1} , vanishes. We can re-write this Eq. as a matrix problem,

$$\mathcal{M}_D \hat{\phi}_n = -\mathcal{M}_Q \hat{\phi}_n; \text{ with } \hat{\phi}_n = \begin{pmatrix} \hat{\phi}_{n,1} \\ \vdots \\ \hat{\phi}_{n,M} \end{pmatrix} \text{ and } \begin{cases} (\mathcal{M}_D)_{l,m} = \frac{d^2}{d\psi_l^2} \mathcal{C}_m(\psi_l), \\ (\mathcal{M}_Q)_{l,m} = \mathcal{Q}_n(\psi_l) \mathcal{C}_m(\psi_l) \end{cases} \quad (7)$$

Then for finding the final solution, search for values of ω in the (ω_r, γ) plane, such that one eigenvalue of the matrix $\mathcal{M} = \mathcal{M}_D + \mathcal{M}_Q$ vanishes within machine precision. For this purpose a method that finds the minimum of a scalar function of several variables, starting at an initial guess value, and iterates using the *simplex search* method [5] is used.

Results

We use this spectral method for global-linear analysis for both the two cases, (i) $H_{eq} \approx E$ and (ii) ψ dependent $H_{eq}(\psi)$. For both the cases we choose similar temperature profile (Fig. 1a),

$$T(\psi) = T_0 + \frac{G_T}{2} \left(1 + L_1 \left[\log \left(\cosh \frac{\psi - \psi_1}{L_1} \right) - \log \left(\cosh \frac{\psi - (1 - \psi_1)}{L_1} \right) \right] \right), \quad (8)$$

with $L_1 = 0.025$, $\psi_1 = 0.1$ and $G_T = 0.19$ for $H_{eq} \approx E$ and $G_T = 1.9$ for ψ dependent $H_{eq}(\psi)$. Also we consider $\kappa_n = 1$ for both the cases. In case of ψ dependent $H_{eq}(\psi)$, the precession frequency profile is chosen as Fig. 1b, and associated $\Lambda_D(\psi)$ profile is obtained from Eq. (2). For $H_{eq} \approx E$ case we choose constant $\Omega_D = 1$ and $\Lambda_D = 1$. The spectral coefficients $\hat{\phi}_{n,m}$ decrease exponentially for both the cases (Fig. 1c), which confirms the spectral convergence of $\hat{\phi}_{n,m}$. In the global linear analysis, $\omega_r \sim 2n$ which is different from the local linear analysis, $\omega_r \sim 3/2n$. The inclusion of the radial profile of drift velocity in the model, the ψ dependent H_{eq} profiles introduces a new parameter κ_Λ in the dispersion relation. Due to this modification real-part of frequency ω_r increases compared to $H_{eq} \approx E$ case (Fig. 1d). In case of ψ dependent $H_{eq}(\psi)$, $\omega_r \sim 10n$ (for $n < 10$) whereas for $H_{eq} \approx E$ case $\omega_r \sim 2n$. κ_Λ term reduces the effect of κ_T and κ_n , whereas for $H_{eq} \approx E$ case, growth-rate (γ) only depends on κ_T ($\kappa_n = 0$). Therefore, relatively a higher temperature gradient is required to obtained equal growth-rate of most unstable mode in case of $H_{eq}(\psi)$, compared to $H_{eq} \approx E$ case. Fig. 1e, present growth-rate profiles for both the cases which agree with a semi-Lagrangian-based linear Vlasov solver TERESA with good accuracy [1]. The potential solution for both the cases is presented in Fig. 1f. In the nonlinear evolution, after the linearly growing phase, the growthrate of TIMs decreases and nonlinear saturation occurs.

References

- [1] D. Mandal, M. Lesur, E. Gravier *et. al.* submitted to Plasma Phys. Cont. Fusion **65**, 055001 (2023)
- [2] V. G. Pryimak and T. Miyazaki, J. Comput. Phys. **142**, 370 (1998)
- [3] G. Depret, X. Garbet, P. Bertrand *et. al* Plasma Phys. Cont. Fusion **42**, 949 (2000)
- [4] E. Gravier and E. Plaut, Phys. Plasmas **20**, 042105 (2013)
- [5] J. C. Lagarias, J. A. Reeds, M. H. Wright, and P. E. Wright, SIAM J. Opt. **9**, 112 (1998).